

Solving the Poisson-Boltzmann Equation to Obtain Interaction Energies Between Confined, Like-charged Cylinders

Mark Ospeck, Seth Fraden

The Complex Fluids Group, Martin Fisher School of Physics, Brandeis University,
Waltham, MA 02454, USA

(July 19, 2018)

We numerically solve the non-linear Poisson-Boltzmann equation for two cylinders confined by two parallel charged plates. The repulsive electrical double layer component of the cylinder pair potential is substantially reduced by confinement between like-charged plates. While the effective cylinder surface charge is increased by the confinement, the effective interaction screening length is reduced, this effect being dominant so that the repulsive confined cylinder-cylinder interaction potential is reduced.

I. INTRODUCTION

Recent experiments have cast doubts that the DLVO pair potential is correctly describing the pair interaction between like-charged colloids in aqueous suspension in a confined region where the colloid motions are being restricted by the confining double layers. Long range attractive potentials of order $1 K_B T$ in strength have been observed [1–5]. Additionally there is interest in whether shorter range interactions between like-charged cylinders in monovalent electrolyte can become attractive under certain circumstances [6–9]. Here we examine the problem of long range interactions between parallel like-charged cylinders confined between like-charged plates by numerically solving the two dimensional, confined, non-linear Poisson-Boltzmann equation.

II. NUMERICALLY SOLVING THE 2D, CONFINED, NON-LINEAR POISSON-BOLTZMANN EQUATION

Two water-solvated like-charged cylinders experience an electrical double layer (EDL) repulsion, their behavior governed by the non-linear Poisson-Boltzmann (PB) equation, which dictates both the potential and simple ion concentration distributions in their vicinity:

$$\nabla^2 \phi = \kappa^2 \sinh \phi \quad (1)$$

Where ∇^2 is the scalar Laplacian operating upon the dimensionless potential ϕ , which equals the scalar potential ψ divided by $K_B T / ze$, with e being the quantum of charge, and z the charge of a single counterion. κ^{-1} is the Debye screening length. Assuming the simple ions to be monovalent $K_B T / ze = 25.69 \text{ mV}$ at 298 K.

The EDL interaction forms the repulsive component of the DLVO potential between two like-charged colloidal particles. At constant thermodynamic volume the Helmholtz free energy is appropriate for describing the EDL interaction between two like-charged colloidal particles. At constant surface potential, the EDL interaction energy has three parts: an attractive electrical term (negative cylinder surface residues attracted to the positive

charge counterion cloud between them), a repulsive entropy term (ion/solvent configurational entropy decreasing with decreasing cylinder separation), and a repulsive chemical potential term (counterion number is decreased by surface charge condensation as the cylinders approach each other). While at constant cylinder surface charge, the EDL has only two parts: an attractive electrical term and a dominant repulsive entropy term (with constant surface charge, counterion number is constant).

The two dimensional problem of circles confined by line charges is equivalent to parallel cylinders confined by walls in three dimensions. Numerical computations of the nonlinear Poisson-Boltzmann (PB) equation were performed principally for two circles of constant (dimensionless) charge density ($\sigma = \frac{d\phi_{\text{circ}}}{d\hat{n}}$ where \hat{n} is the normal to the surface) confined by two constant (dimensionless) potential line charges (ϕ_{line}) as sketched in Fig. 1. The boundary condition was usually constant charge on the cylinders and always constant potential on the confining charged walls because we supposed the cylinders to possess strong acid groups, typical of surface groups such as polystyrene sulfonate, while we assumed the confining walls were made of glass, which contains a high density of weak acid silanol groups.

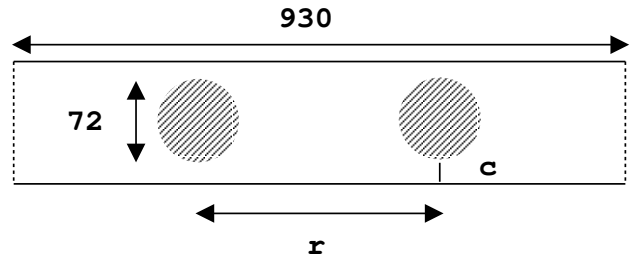


FIG. 1. Geometry for solving the 2d, confined, non-linear Poisson-Boltzmann equation. Lengths are in grids of a 2d square lattice, where the reservoir, or bulk screening length is 6-30 grids. Typically, a constant potential boundary condition (b.c.) is imposed on the confining line charges, a constant charge (potential slope) b.c. is imposed on the circles, and a free b.c. is employed at the left and right boundaries of the space (extrapolating the local potential slope, which equals zero far from the circles). The space's width was chosen so that the circle-circle interaction potentials were insensitive to increases in width. c is the closest distance between the circle and the line, and r is the center-center separation between the circles, all in grids.

Our use of a constant potential glass boundary condition needs further clarification. This is a standard low surface potential, weak acid surface group boundary condition [10] and is enforced at the outer Helmholtz plane (OHP) where the compact, or Stern layer ends, and by association dissociation equilibria of weak acid surface groups and also two dimensional mobility of counterions within the compact layer. This layer is a highly concentrated monolayer of aqueous counterions typically containing 90 percent of the glass countercharge and well over 100 millivolts of potential change so that the resulting glass boundary condition which faces the electrolyte at the OHP is a low (usually well less than 100 millivolt) constant potential [10,17]. Our results depend upon this glass regulating constant potential boundary condition's ability to stand up under compression. Should it fail then there would follow electric field lines leaking into the low dielectric glass and polarizing electron clouds. It would then become important to account for unscreened interactions between these polarized electron clouds. This paper discusses the limited constant potential confining boundary case. A complete treatment would include the field inside the glass, model the glass-water interface with a regularizing boundary condition [16], as well as calculating the field between the charged circles. Although it is expected that the constant potential glass boundary condition would remain valid at compressions between surfaces down to one screening length [15] there is some evidence that under extreme compression it is in fact the case that field lines are traversing through the external dielectric [3]. The inclusion of regularizing boundary conditions [16] is a direction for future research.

There is zero electric field within the circles. Note that the constant surface charge boundary condition on the circles will not be a problem because field line penetration into the low dielectric circles causes only a small perturbation in the circle-circle interaction (see Fig.9).

A periodic boundary condition was employed at the left and right edges of the space (at these edges we extrapolated the local potential slope in the direction parallel to the confining lines, which was equal to zero, since these boundaries were many tens of screening lengths separated from the circle edges; see Fig.4). The space's width was chosen so that the circle-circle interaction potentials were

insensitive to increases in this width.

The geometrical details of our numerical simulation are as follows. Our circle's radius a was fixed at 36 grids of a 2d square lattice, the screening length κ^{-1} varied from 6 to 30 grids, while the space was made 930 grids in length in order to avoid edge effects. The distance from the circle's surface to the line charge c was varied from 6 to $\frac{1}{2}$ screening lengths. Venturing much below $\kappa c = \frac{1}{2}$ was found to introduce coarse graining errors, and a more sophisticated multi-grid relaxation algorithm [12] would be necessary in order to accurately track the highly curved potential function in this very strongly confined regime. Potential fields for fixed circle and line boundary conditions, c , and κ^{-1} were obtained by numerically solving the non-linear Poisson-Boltzmann equation on a Silicon Graphics work station having a MIPS R4400 processor, and by using a successive overrelaxation (SOR) [12] algorithm, employing an SOR factor of 1.85. Total free energies TFE for a given separation r were obtained via the Helmholtz prescription from Overbeek [11], so that a circle-circle interaction potential could subsequently be constructed. Then we made a two parameter fit of the Helmholtz interaction energy to

$$V_{EDL,2D} = \frac{Z^2}{L^2} GF \frac{e^{-\kappa_{local} r}}{\sqrt{r}}, \quad (2)$$

$\frac{Z}{L}$ being the cylinder's charge per unit length. The fit netted κ_{local}^{-1} and a geometric prefactor GF depending upon local screening length and particle radius. Between spheres in three dimensions [13]

$$GF_{3D} = \frac{e^{\kappa_{local} 2a}}{(1 + \kappa_{local} a)^2}, \quad (3)$$

while between cylinders in two dimensions

$$GF_{2D} = \frac{e^{\kappa_{local} 2a}}{(1 + 2\kappa_{local} a)^2}. \quad (4)$$

These fits revealed that use of the bulk screening length κ^{-1} was not appropriate for the confined circle-circle interaction. As the circles were increasingly confined by the line charges the circle-circle interaction's effective screening length was found to decrease in a systematic way, with the line charge counterions screening the circle-circle interaction. In addition, the circle's effective charge $\frac{Z}{L} \sqrt{GF}$ was found to be increased by the confinement.

Overbeek's Free Energy bookkeeping [11] goes as follows:

$$\text{Total Free Energy} = TFE = EFE + CFE \quad (5)$$

$$EFE = \text{Electrical Free Energy} = EE - T\Delta S \quad (6)$$

$$\begin{aligned} CFE^* &= \text{Chemical Free Energy}^* = \\ &= -2 \int_S (\phi \frac{d\phi}{dn}) dS \\ &= -2 \int_A ((\nabla\phi)^2 + \kappa^2 \phi \sinh \phi) dA \end{aligned} \quad (7)$$

$$EE^* = \text{Electrical Energy}^* = \int_A (\nabla\phi)^2 dA \quad (8)$$

$$T\Delta S^* = -2\kappa^2 \int_A (1 - \cosh\phi + \phi \sinh\phi) dA \quad (9)$$

Where * indicates a dimensionless 2d energy, dS represents a small element of constant potential boundary, and dA a small area of electrolyte. Converting a 2d dimensionless free energy into a 3d dimensionfull one requires multiplying by $k_B T$, by $\frac{1}{4\pi}$, and by one half the number of Bjerrum lengths the circular cylinders extend into the z direction [14]. Take Fig. 2 as an example: if its cylinders were 500nm in radius, $\kappa^{-1}=280\text{nm}$ (in order that $\kappa a=1.8$), and the cylinders were 1000nm in length, then we should multiply their dimensionless 2d energies by $k_B T \frac{1}{4\pi} \frac{1000\text{nm}}{1.4\text{nm}} = 57 k_B T$, i.e. at $\kappa r=10$, $\kappa c=6$ the cylinders would experience about a 0.6 $k_B T$ repulsion. The free energies obtained from numerical solutions of the PB for interacting flat plates compared well against the tabulated values in the Verwey-Overbeek monograph [17], and also against Israelachvili's figure 12.10 [15].

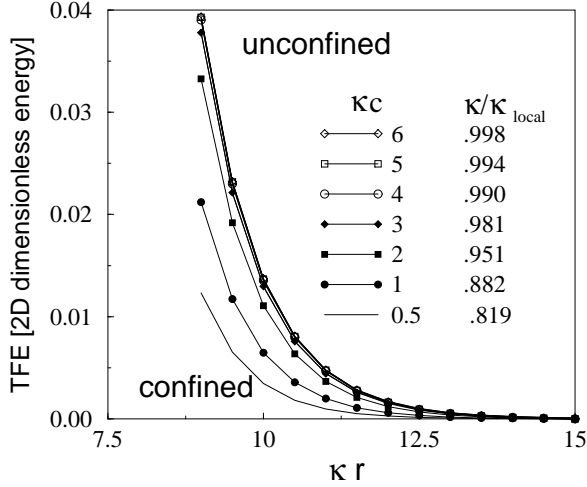


FIG. 2. Reduction of interparticle repulsion between a pair of charged rods due to the rods being confined by a pair of charged plates. 2d dimensionless total free energies TFE versus circle-circle separations κr for the case where inverse screening length times circle radius $\kappa a=1.8$, and as a function of circle edge-line separation κc . Note that in order to obtain a three dimensional free energy one must multiply TFE by $\frac{k_B T}{4\pi}$ and by the number of Bjerrum lengths the circular cylinders extend into the z direction. The circle boundary condition (b.c.) is .0507 constant potential slope (corresponding to a -1 free surface potential if $\kappa a=1.8$) and the confining line b.c. is -2 constant potential. Lines are two parameter fits of the data points to Eq. 2, thereby obtaining the geometric factor GF and κ_{local}^{-1} as a function of circle edge-line separation κc . The repulsive interaction is substantially reduced and the local Debye screening length is shortened by the presence of the charged plates.

Figure 2 shows seven EDL potential barriers between

two circles confined by line charges arranged in the geometry depicted in Fig.4. The dimensionless total free energy TFE (Eqs.5-9) is plotted versus the circle's center to center separation r . The circles have a free potential equal to -1, but it is their surface charges which are held constant during the circle-circle interaction, this because the circle surfaces are assumed to possess strong acid groups which resist charge condensation. Their constant potential slopes are equal to .0507, the appropriate slope for a -1 potential free surface when $\kappa a=1.8$, i.e. the screening length is 20 grids, and the circle's radius a is fixed at 36 grids. Here the confining line charges are held at constant -2. potential, and are thus said to be perfectly regulating because their surfaces are assumed to be composed out of weak acid groups. Circle edge-line charge separation c is varied from $\frac{1}{2}$ to $6 \kappa^{-1}$. Circle motion is assumed to be adiabatically cut off from the motion of the ion gas, i.e. the ions are assumed to readjust to the new circle configurations with extreme rapidity. Circle separation r begins at $15\kappa^{-1}$ and is decremented by units of $.5 \kappa^{-1}$ down to $9 \kappa^{-1}$, all the while solving the PB equation and subsequently recording the configuration's Helmholtz free energy TFE . A two parameter fit of the (r, TFE) data points is made to the 2d EDL potential function (Eq.2), thereby obtaining the interaction screening length κ_{local}^{-1} , and observing that this circle-circle interaction screening length is decreased from the bulk value by close confinement of the line charges.

Figure 3 breaks down the relative contributions made to the circle-circle interaction potential between the electrical, entropic, and chemical free energies (Eqs.5-9) for Fig.2's case of strongly confined circles. The case of two constant potential line charges confining two constant charge circles contains two attractive and one repulsive terms. The smaller of the attractive terms is the chemical free energy term (the number of *line-charge* counterions increasing as the circles move together). The larger attractive term is electrical in origin arising from the counterions located in between the two circles—like in a hydrogen molecule. However, at 300 Kelvin, the repulsive entropic term dominates the attractive terms.

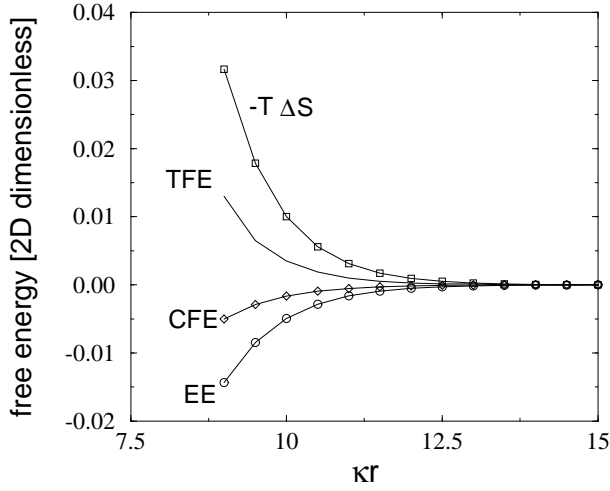


FIG. 3. The three component terms of the circle-circle interaction free energy for Fig.2's case of strong confinement are plotted versus circle center-center separation κr , where EE is electrical energy, always attractive, $-T\Delta S$ due to ion/solvent configurational entropy, always repulsive, and CFE is a weak attractive chemical free energy (line charge counterion number increases when circles are close together). Notice that the repulsive ion/solvent configurational entropy term is dominant, meaning that the total potential is repulsive and that this repulsion is due to osmotic pressure forces. The conditions are two constant -2 potential line charges strongly confining ($\kappa c=.5$) two interacting constant potential slope circles (.0507 slope appropriate to a free -1 potential if $\kappa a = 1.8$).

Figure 4 shows three contour plots associated with Fig.2 and appropriate to greater or lesser degrees of confinement. When the circles are more confined the contours surrounding each circle become more elongated, reflecting the fact that many of the circle's electric field lines are now terminating locally in the line charge's double layer. One could think as if the field lines were terminating in partial image charges created in the line charge double layer.

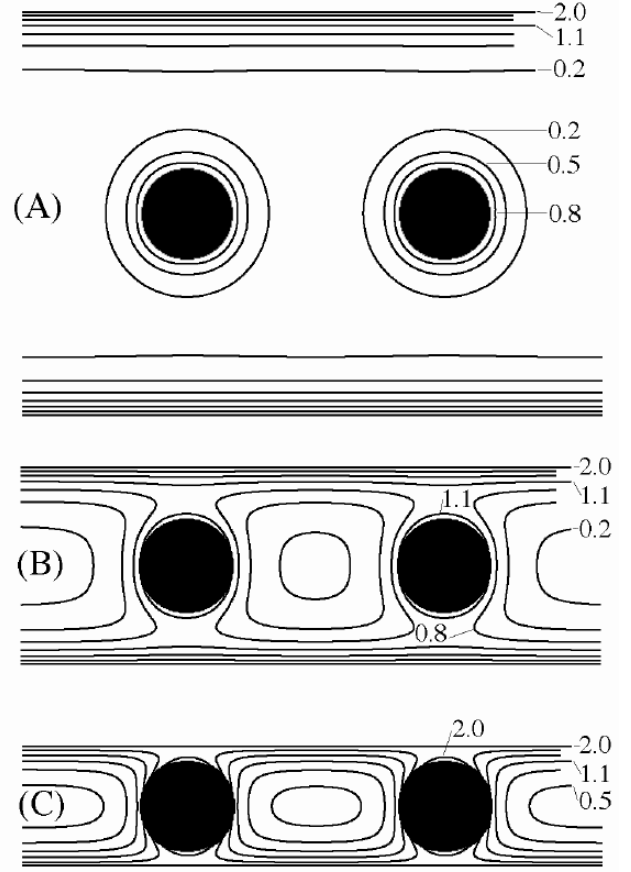


FIG. 4. Contour plots of the dimensionless potential (ϕ) for the conditions shown in Fig.2. The circles have constant charge (their boundary potential slope which equals .0507 corresponds to an unconfined potential equal to -1 when $\kappa a=1.8$) and the line charges are at constant -2 potential. All potentials are negative. $\kappa r=10$ for all three plots. There is no electric field within the black circle interiors. (a) The circle-circle interaction is virtually undisturbed by the distant charged lines, $\kappa c=6$. (b) The circle-circle interaction is becoming weakened by confinement, $\kappa c=2$. Note the increasing circle surface potential. (c) Strong confinement, $\kappa c=.5$. Field lines normally involved in the circle-circle repulsive interaction are being redirected, terminating on the counterions in the charged line's double layer.

Figures 5,6, and 7 are all connected. In Fig.5 the confining line potential is increased to -6 and the confined circle-circle interaction screening length κ_{local}^{-1} is appreciably lessened when compared with Fig.2 which has only a -2 potential confining line. The large line capacitance is acting to hide the circles from each other. Figure 6 gives the relationship between confining line potential and local screening length, while Fig.7 shows for a free *line charge* the relationship between confining line potential ϕ_{line} and line capacitance per unit length C/L .

$$C/L = \frac{\left(\frac{d\phi_{line}}{d\eta}\right)}{\phi_{line}} \quad (10)$$

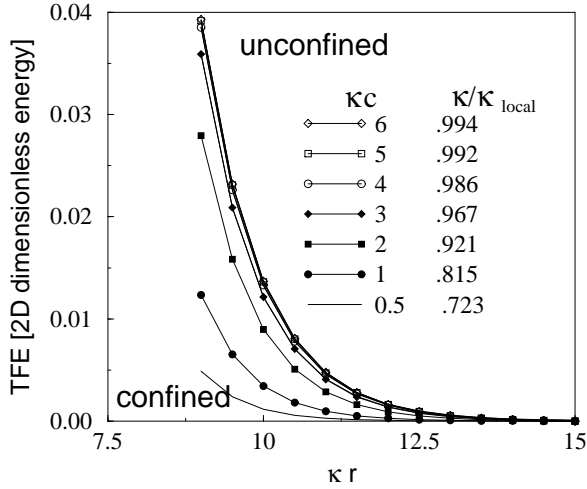


FIG. 5. Reduction of interparticle repulsion by increasing the confining potentials compared to Fig.2. Plots of total free energy TFE versus circle-circle separation (κr) for .0507 constant potential slope circles confined by line charges held at a -6 potential, and $\kappa a=1.8$. The circle-circle barrier potential is reduced by approximately one order of magnitude when the circles are severely confined. Note that the degree of confinement κc is varied from 6 to $\frac{1}{2}$.

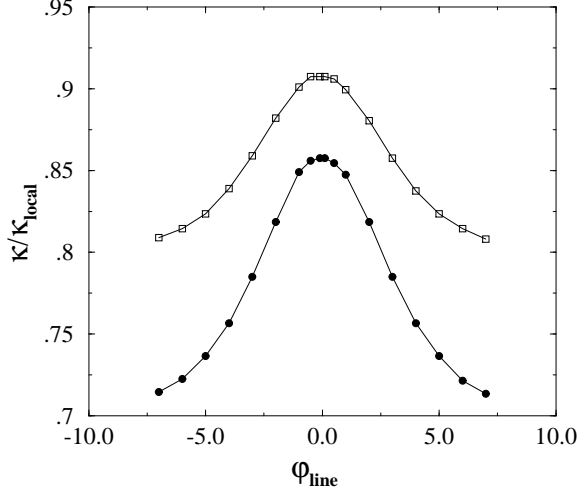


FIG. 6. The ratio of local screening length κ_{local}^{-1} to bulk screening length κ^{-1} as a function of the confining line potential ϕ_{line} boundary condition. The curve is symmetric with respect to the confining line potential. The conditions are $\kappa a=1.8$, solid circles correspond to $\kappa c = .5$ (strong confinement), hollow squares to $\kappa c = 1$ (weaker confinement), while the circles have constant (charge) potential slope $=.0507$.

Figure 7's potential slope fits the Grahame equation [15]

$$\frac{d\phi}{d\tilde{n}} = \kappa 2 \sinh \frac{\phi}{2}. \quad (11)$$

Also note Fig.7 capacitance per unit length's nonzero y-intercept ($\approx .05 = \kappa$) shows that line capacitance goes

like inverse screening length κ for a free line when ϕ_{line} is held at zero potential (obtained by dividing the r.h.s. of the Grahame equation by ϕ_{line} , while taking the limit as $\phi_{line} \rightarrow 0$). In Fig.6 we plotted local screening length versus confining line potential and obtained gaussian functions symmetric about the zero of potential. Notice that the local screening length is $.85\kappa^{-1}$ for zero potential line charges strongly confining the circle-circle interaction, $\kappa c=.5$, and that this is connected with the fact that a zero potential confining line charge possesses an increased capacitance determined by a Grahame equation modified to account for the confinement [16]. Essentially, strong confinement brings the zero potential line an additional capacitance due to its sharing of the confined circle's counterions. Interestingly, the local interaction screening length is independent of the sign of the surface charge on the confining lines. Apparently as regards the local screening length it does not matter if a negative field line sourced from a circle terminates in the line's double layer on a positive counterion or on the positive line charge itself.

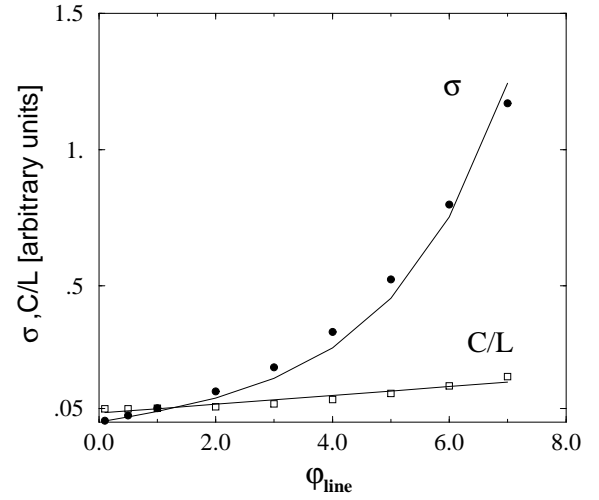


FIG. 7. Plots for a free *line charge* of its boundary potential slope $\sigma (= \frac{d\phi_{line}}{d\tilde{n}}$, solid circles) and its intrinsic capacitance per unit length $C/L (= \frac{\sigma}{\phi_{line}}$, hollow squares; see Eq.10) versus free line potential ϕ_{line} . The line tracing the solid circles is a fit to the Grahame equation (Eq.11).

The second Eq.2 fitting parameter GF stands for the DLVO *geometric factor* [13], which accounts for the internal volume of the cylinder being excluded to the screening ions. For a typical colloidal particle there are two effects competing to set effective surface charge $Z\sqrt{GF}$ as one increases the concentration of potential determining ions (p.d.i.). A p.d.i. electrolyte is contrasted to an indifferent electrolyte, the distinction being that an indifferent electrolyte is unable to bind to surface residues. The first effect concerns binding of a p.d.i. to a surface residue, thereby decreasing Z , while the second occurs

as the concentration gradient of p.d.i.'s in the vicinity of a charged surface is increased, thus making the particle appear to have increased its surface charge. This second effect is the one accounted for by DLVO's GF . If one holds Z constant while increasing ionic strength, then one observes an increasing effective particle surface charge $Z^* = Z\sqrt{GF}$ due to the steepened counterion concentration gradient. We see in Fig.8 that GF increases in a gaussian fashion with increasingly negative confining line potential. Compare the behaviors of the two fitting parameters GF (Fig.8) and κ_{local}^{-1} (Fig.6). Local screening length doesn't care about the sign of the surrounding line charge, but GF certainly does.

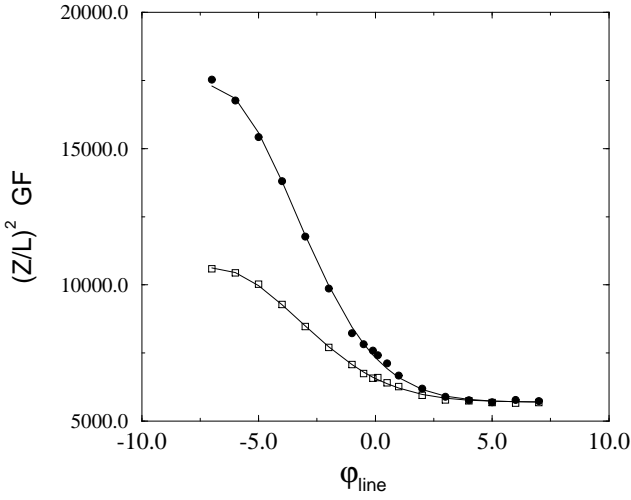


FIG. 8. Plot of $\frac{Z^2}{L^2} GF = \frac{Z^{*2}}{L^2}$ versus line potential ϕ_{line} for two confined interacting .0507 constant potential slope circles when $\kappa a = 1.8$. $\frac{Z^*}{L}$ is the effective surface charge on the circle. The solid circular data points correspond to $\kappa c = .5$ (strong confinement), and the hollow squares to $\kappa c = 1$ (weaker confinement).

After κ_{local}^{-1} as a function of c is obtained from Eq.2 (see Figs.2 and 5) we make a one parameter fit to the function

$$\kappa_{local}^{-1} = \kappa^{-1} e^{-Ae^{-\kappa c}} \quad (12)$$

and plot the result in Fig.9. Local screening length goes like the inverse square root of local ionic strength ($\kappa_{local}^{-1} \sim n^{-.5}$), which itself goes like an exponential function of the local potential (Boltzmann factor: $n \sim e^{-\phi}$), and finally this local potential goes like a decaying exponential function of distance from a charged surface ($\phi \sim e^{-\kappa c}$).

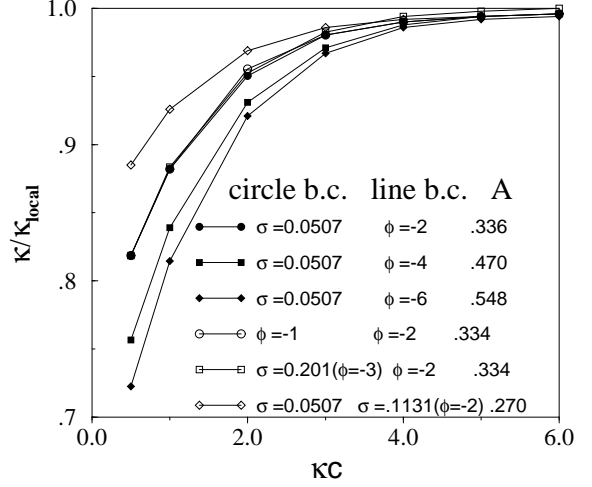


FIG. 9. Local screening length versus the confinement distance between the circle and the line charge, κc , for various circle and line boundary conditions, where $\phi = \frac{\psi}{K_B T/e}$ is a dimensionless surface potential boundary condition (b.c.) and $\sigma = \frac{d\phi}{dn}$ a surface charge b.c., and with $\kappa a = 1.8$. The lines are one parameter fits to the factor A in Eq.12. The solid data points demonstrate the line potential's control over the local screening length. Meanwhile changing the circle b.c. had little effect on interaction screening length, as seen by comparing the solid circle, open circle, and open square data sets. Note that a constant charge b.c. on the confining plate corresponding to a -2 potential, i.e. the open diamond ($A = .270$) had a significantly smaller effect on local screening length than did its -2 confining potential counterpart. This probably had to do with the fact that *line charge* counterion number increased when the circles were close together, for the case of constant potential confining lines (see Fig.3).

Fig.10 shows that decreasing c , i.e. increasing the degree of confinement, increases the GF for all of the constant-charge circle-circle interactions. In contrast, for the case of confined constant-potential circles the square data points show that the combination $\frac{Z^2}{L^2} GF$ actually decreases. For strong confinement (small c) condensation of counterions decreases the circle's surface charge $\frac{Z}{L}$, and this effect wins out over an increasing GF .

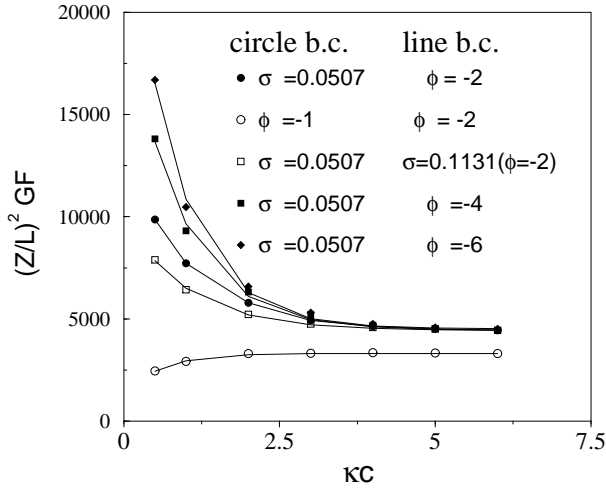


FIG. 10. Squared surface charge per unit length times the DLVO *geometric factor* $\frac{Z^2}{L^2} GF$ (see Eq.2) versus confinement κc for various circle and line boundary conditions, where $\phi = \frac{\psi}{K_B T/e}$ is a dimensionless surface potential b.c., $\sigma = \frac{d\phi}{dn}$ a surface charge b.c., and $\kappa a = 1.8$. Only in the constant potential circle case where surface charge regulation acts to decrease Z does $\frac{Z^2}{L^2} GF$ decrease with increasing confinement.

Finally we vary bulk screening length from 6 grids to 30 grids for various amounts of confinement, and obtain the dependence of local screening length on bulk screening length for these differing degrees of confinement (Fig.11). In our 2d geometry there are 3 independent length scales : circle radius (fixed at 36 grids), circle edge-line separation c (varying from 10 to 40 grids), and κ^{-1} (varying from 6 to 30 grids, i.e. κa decreases from 6 to 1.2). The circle-circle interaction's length scale κ_{local}^{-1} is a function of these three. As one increases the bulk screening length one decreases the space's midplane potential towards the line potential ($\phi_{line} = -2$ in Fig.11), and thus more of the circle's field lines traverse a region where the local ionic strength has been increased by a factor of $\cosh[-2] = 3.76$ times the bulk ionic strength (counterions increased by the factor e^2 while the coions decrease by e^{-2}). Hence the screening length "seen" by these field lines will be reduced by a factor $\frac{1}{\sqrt{3.76}} = .52$. While for the case $\kappa^{-1} = 6$ most of the interaction field lines sample electrolyte where $\kappa_{local}^{-1} = \kappa^{-1}$.

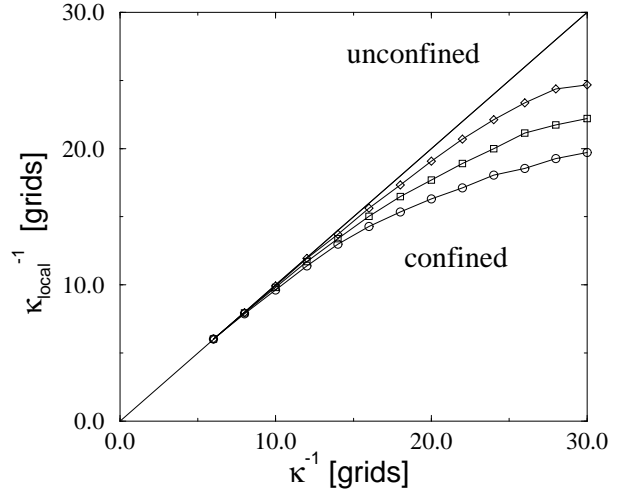


FIG. 11. Local screening length κ_{local}^{-1} as a function of bulk screening length for various degrees of confinement. The circles have a constant potential slope $=.0507$ (corresponding to a -1 free surface potential only when $\kappa a = 1.8$) and the line charges are held at a -2 potential. Local screening lengths were obtained by a fit to Eq.2 of the total free energies in a region where circle surface to surface separation was approximately 5.5 bulk screening lengths. The diagonal corresponds to $\kappa_{local}^{-1} = \kappa^{-1}$, open circles to $c=10$ grids, open squares to $c=20$ grids, open diamonds to $c=40$ grids, while the circle radius is 36 grids. The local screening length increases to the bulk screening length as the confining line charges move apart.

Solutions to the confined non-linear Poisson-Boltzmann equation for like- charged cylinders appear to be repulsive, screened, Yukawa-like potentials, having an effective screening length κ_{local}^{-1} which is found to be a decreasing function of increasing confinement. The effective charge of the cylinders $Z^* = \frac{Z}{L} \sqrt{GF}$ is found to be an increasing function of increasing confinement.

III. CONCLUSIONS

By numerically solving the two dimensional, non-linear, confined Poisson-Boltzmann equation we've found that the electrical double layer (EDL) repulsion can be significantly decreased between two parallel cylinders when confined between two charged plates because the confining double layers constitute a high capacitance region which screens the cylinder-cylinder interaction.

ACKNOWLEDGMENTS We thank the referee for numerous suggestions for clarifying the text. This research was supported by DOE DE-FG02-87ER45084.

-
- [1] G.M.Kepler and S.Fraden, Phys.Rev.Lett. **73**, 356(1994).
 - [2] J.C.Crocker and D.G.Grier, Phys.Rev.Lett.**73**, 352(1994).
 - [3] J.C.Crocker,D.Grier, Phys.Rev.Lett. **77** ,1987(1996).

- [4] A.E.Larsen,D.G.Grier,Nature **385** , 230(1997).
- [5] M.D.Carbajal-Tinoco,F.Castro-Román,J.L.Arauz-Lara,Phys.Rev.E,**53** ,3745(Apr 1996).
- [6] V.A. Bloomfield, Biopolymers **31** ,1471 (1991).
- [7] R.Podgornik,D.Rau,and V.A.Parsegian, Biophys. J. **66** ,962(1994).
- [8] J.X.Tang,S.Wong,P.Tran, and P.Janmey, Ber.Bunsen-Ges.Phys.Chem. **100** ,1(1996).
- [9] N.Gronbech-Jensen,R.J.Mashl,R.F.Bruinsma,W.M.Gelbart,Phys.Rev.Lett.**78** ,2477(1997).
- [10] H.E.Bergna Ed., “The Colloid Chemistry of Silica”, Advances in Chemitry 234 (1994, American Chemical Society).
- [11] J.T.G.Overbeek,Colloids and Surfaces,**51**,61-75(1990).
- [12] W.H.Press,S.A.Teukolsky,B.P.Flannery,W.T.Vetterling, “Numerical Recipes in C”,Cambridge Univ.Press(1988).
- [13] A.K.Sood,Solid State Physics **45** , 1(1991).
- [14] A.K.Sengupta,K.D.Papadopoulos,Journal of Colloid and Interface Science,**149**,135(1 March 1992).
- [15] J.N.Israelachvili, “Intermolecular and Surface Forces”,Academic Press (1985).
- [16] D.Y.C.Chan,R.M.Pashley,L.R.White,Journal of Colloid and Interface Science,**77**,283(Sept 1980).
- [17] E.J.W.Verwey, J.TH.G.Overbeek, “Theory of the Stability of Lyophobic Colloids”, pp.195-199, Elsevier Publishing Co.,inc.,New York (1948).